ISO BEAM PROFILES AND EXTENDED SOURCE FLUX CALIBRATION

A. Salama

ISO Data Centre, ESA Astrophysics Division, Villafranca del Castillo, P.O. Box 50727, 28080 Madrid, Spain

ABSTRACT

The methodology to derive surface brightness for ISO data via the beam profiles is briefly described. An overview of the status for the four instruments is given.

Key words: ISO; beam profile; PSF; surface brightness; flux calibration.

1. INTRODUCTION

The flux calibration of the ISO instruments has been derived on the basis of point–like calibration sources. For an extended source, the flux is defined in terms of flux per unit solid angle on the sky. In the ideal case of an infinitely extended and homogeneously distributed source, the surface brightness is in principle the flux seen by the instrument, divided by effective beam (or rather beam solid angle Ω_{eff}). The effective beam can be derived from the beam profile: it is equal to the profile integral divided by the profile height at the position for which the point-source calibration applies. For sources with spatial structure, the point source calibration applies to the convolution of the source brightness distribution with the beam profile. Spatial deconvolution requires either a well-observed source map or a reliable model of the source geometry. For simplicity, in this paper we will restrict ourselves to the case of an infinitely extended and homogeneously distributed source and review the status of the extended source flux calibration for the four ISO instruments, excluding the details associated with the characterisation of the instruments' beam profiles. Currently available conversion factors from point source to extended source flux calibration are presented for illustration. These numbers are included (or will be) in the ISO instruments' automatic processing pipeline (OLP) calibration files. The reader is adviced to use the values contained in the most recent version of the OLP available at the time of reading.

1.1. Surface brightness derivation

The flux calibration of the ISO instruments has been derived by positioning well known calibration point-like sources at the nominal centre of the instrument aperture or detector pixel, and relating the detector signal from the astronomical calibration source with the signal obtained from the internal calibration sources. Not all the flux from the point-like flux calibration source collected by the telescope area will reach the detector, due to diffraction. The fraction of flux measured by the detector (hereby called f_{PSF}) can be obtained ideally by convolving the telescope optical system Point Spread Function (PSF), normalised to an area of one, with the instrument apertures and detector response profiles (neglegting for simplicity transmission losses, interference caused by parallel surfaces in the instrument, etc.). The *beam profile* is here defined as the map obtained by moving the point–like source across the aperture.

The derivation of extended source flux from a point source calibration may be expressed as follows, if we think of an extended source as composed of an infinite number of point sources:

$$I_\nu = \frac{F_\nu}{\int_{-\infty}^{+\infty} BP(y,z)\, dydz} \quad (\mathrm{MJy\,sr^{-1}}) \qquad (1)$$

where F_ν is the (point-source) flux density at the frequency ν and $BP(y,z)$ is the detector's Beam Profile, normalised to the value at the position in which the flux calibration has been derived, nominally the (0,0) position. The variables y and z are angles with respect to the spacecraft Z and Y axes.

In the case of LWS and PHT, the integral over the beam profile (i.e. the denominator in Equation 1) is performed over the beam profile before normalisation. Subsequently, the normalisation is performed by dividing the integral by f_{PSF} which is the fraction of the total point source flux falling on a given detector pixel at the nominal position (0,0) used for the point source flux calibration. This may also be expressed as the

$$\int_{-\infty}^{+\infty} BP(y,z)\, dydz = \Omega_{eff}/f_{PSF} \quad (\mathrm{sr}), \qquad (2)$$

where Ω_{eff} is the effective solid angle of a detector pixel.

"ISO Beyond Point Sources: Studies of Extended Infrared Emission", Madrid, Spain, 14–17 Sep 1999 (ESA SP-455, April 2000)

2. LWS

The characterisation of the LWS beam profile is described in Lloyd (2000) and Gry et al. (2000). The LWS surface brightness is derived by splitting the beam integral in two parts – the geometrical effective solid angle Ω_{eff}, obtained from the width of the mean beam profile, and the fraction of the ISO telescope Point Spread Function (PSF) going into this aperture f_{PSF} (the rest is lost due to diffraction). Equation 1 becomes:

$$I_\nu = \frac{F_\nu f_{PSF}}{\Omega_{eff}} \quad (\mathrm{MJy\,sr^{-1}}) \tag{3}$$

The LWS beam profiles have been derived by convolving an Airy profile with inflated wings (mimicking the ISO PSF) with the detector instrumental profile, assumed to be circular, with a radius of 40″ and a rectangular response. The derived effective solid angles and f_{PSF} for each LWS detector are listed in Table 1. Current developments in the LWS extended source calibration include the use of the ISO telescope PSF model (Okumura 2000), a more realistic geometry for the apertures and defringing the beam profile calibration data. The parameters describing the LWS beam profile and the conversion from point to extended source fluxes are planned for inclusion in ISAP 2.0 and OLP V10 as standalone calibration files.

Table 1. LWS Extended source flux derivation parameters

Detector	f_{PSF}	Ω_{eff} ($\times 10^{-7}$ sr)
SW1	0.86	1.07
SW2	0.85	1.18
SW3	0.83	1.30
SW4	0.73	1.30
SW5	0.68	1.24
LW1	0.67	1.18
LW2	0.64	1.24
LW3	0.64	0.90
LW4	0.58	0.66
LW5	0.51	0.66

3. PHT

3.1. PHT-C

The PHT-C surface brightness for single pointing observations is derived from the in-band powers of each pixel. For consistency, the computation for PHT-C may be written here as:

$$I_\nu = \frac{F_\nu f_{PSF}}{(1-\epsilon^2)\Omega_{eff} n_{pix}} \quad (\mathrm{MJy\,sr^{-1}}) \tag{4}$$

where F_ν is the flux density at frequency ν seen by the array, n_{pix} is the number of pixels per array (9 for C100, 4 for C200), Ω_{eff} is the solid angle defined per pixel and f_{PSF} is the fraction of source flux seen by the array. For C100 chopped observations however (PHT22), only the central pixel is used, therefore $n_{pix} = 1$ and $f_{PSF} = f_{PSF}^{pixel}$. Similarly, in the case of raster maps, the surface brightness is computed per pixel for each C100 or C200 detector pixel before map coaddition.

The effective solid angles of the C100 and C200 detector pixels Ω_{eff} for each filter band have been computed using a model of the detector beam profile, which takes into account the ISO primary mirror, secondary mirror, tripod, and the linear sizes of the detectors as measured pre-flight. The f_{PSF}'s have been derived empirically from calibration observations of point sources on specific positions in the array (Laureijs 1999), as the model did not take into account the losses at the gaps between pixels. These are stored in standalone calibration files within the processing pipeline (OLP) and are listed in Table 2.

Table 2. Intensity fraction of a point source entering the PHT-C arrays, empirically determined (OLP V8.4 CAL G PCPSF.FITS)

Array	filter	On array centre	On pixel
C100	50	0.828	0.68
	60	0.809	0.69
	70	0.872	0.66
	90	0.791	0.61
	100	0.773	0.57
	105	0.778	0.55
C200	120	0.498	0.69
	135	0.568	0.66
	160	0.528	0.64
	180	0.612	0.62
	200	0.693	0.59

The geometrical solid angles of the pixels are slightly filter dependent, their averages are:

$\Omega_{C100} = 0.0688\times10^{-6}$ sr
$\Omega_{C200} = 0.281\times10^{-6}$ sr.

3.2. PHT-P

The conversion from point source flux F_ν in Jy to surface brightness can be written for a given PHT-P filter as follows (Laureijs et al. 2000):

$$I_\nu = \frac{F_\nu f_{PSF}}{(1-\epsilon^2)\Omega_{eff}} \quad (\mathrm{MJy\,sr^{-1}}) \tag{5}$$

where ϵ is the obscuration factor (1/3) for the ISO secondary mirror. Ω_{eff} (in sr) is the effective solid angle of the aperture, for a given filter, and corresponds to the area of the aperture in the focal plane projected on the sky, determined from the measured physical dimensions of the apertures. The PHT-P beam profiles have been calculated using a simplified model of the ISO telescope PSF, which assumes a uniformly illuminated round mirror of 30 cm radius with an f/15 focal length and a central obscuration of 10 cm radius due to the secondary mirror. The sizes of the apertures and detectors as determined

Table 3. Intensity fraction of a point source entering the apertures of PHT-P (OLP V8.4 CALG PPPSF.FITS and PPOMEGA.FITS).

	PHT-P apertures												
filter	5″	7.6″	10″	13.8″	18″	23″	20×32″	52″	79″	99″	120″	127×127″	180″
P1													
3.29	0.88	0.91	0.94	0.95	0.97	0.97	0.97	0.99	0.99	0.99	0.99	1.00	1.00
3.6	0.84	0.91	0.93	0.95	0.96	0.97	0.97	0.99	0.99	0.99	0.99	0.99	1.00
4.8	0.70	0.90	0.90	0.93	0.95	0.96	0.96	0.98	0.99	0.99	0.99	0.99	0.99
7.3	–	0.77	0.89	0.90	0.92	0.93	0.94	0.97	0.98	0.99	0.99	0.99	0.99
7.7	–	0.74	0.88	0.90	0.91	0.93	0.94	0.97	0.98	0.98	0.99	0.99	0.99
10	–	–	0.75	0.88	0.90	0.91	0.92	0.96	0.97	0.98	0.98	0.99	0.99
11.3	–	–	0.70	0.82	0.90	0.90	0.91	0.96	0.97	0.98	0.98	0.98	0.99
12	–	–	0.69	0.78	0.90	0.90	0.91	0.95	0.97	0.98	0.98	0.98	0.99
12.8	–	–	0.68	0.75	0.89	0.90	0.91	0.95	0.97	0.97	0.98	0.98	0.99
15	–	–	–	0.69	0.84	0.90	0.89	0.95	0.96	0.97	0.97	0.98	0.98
P2													
20	–	–	–	–	0.70	0.78	0.82	0.92	0.95	0.96	0.97	0.97	0.98
25	–	–	–	–	–	0.69	0.77	0.90	0.93	0.95	0.96	0.96	0.97
P3													
60	–	–	–	–	–	–	–	0.69	0.85	0.90	0.90	0.91	0.93
100	–	–	–	–	–	–	–	–	0.68	0.71	0.81	0.87	0.90
Ω ($\times 10^{-8}$ sr)	0.039	0.124	0.214	0.349	0.625	0.97	1.39	5.13	11.21	17.93	26.22	37.3	59.8

on ground, together with the central wavelength of each filter have been used to determine f_{PSF}. These quantities are stored in standalone calibration files within the processing pipeline (OLP) and are listed in Table 3.

3.3. PHT-S

For PHT-S the values of Ω_{eff} for each pixel were determined from in-flight calibration observations of the detector footprints. These values are included in the conversion from signal to extended source flux density. For consistency, in Figure 1 the ratio between point source and extended source calibration curves is plotted.

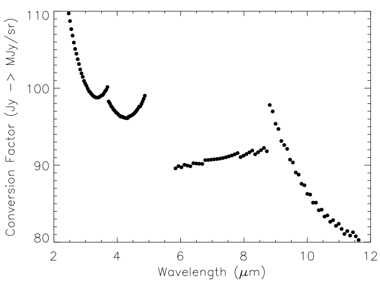

Figure 1. PHT-S point to extended source conversion factors (from OLP V8.4 CALG PSPECAL.FITS)

4. CAM

The characterisation of the CAM PSF is described in Okumura (2000) and Siebenmorgen et al. (2000). The ISOCAM flux calibration is based on the point source photometry, which is performed by a circular aperture photometry along with the aperture correction based on a computed PSF. This correction aims to retrieve all the flux of the point source CAM would see, if the detectors were large enough to sum all the energy spread out by the telescope and the CAM instrument. In this way, after passing from the instrumental unit to Jy, each pixel is assigned a flux density value in Jy/pixel. The surface brightness is then directly derived by changing units, from pixel size in arcseconds to steradiants.

Table 4. CAM Flux conversion factors for extended sources

Pixel Size (arcsec)	Jy to MJy sr^{-1}
1.5	18910
3	4727
6	1182
12	295

5. SWS

The characterisation of the SWS beam profiles is described in Salama (1998). A number of maps around point sources have been used in conjunction with a model which follows the theoretical telescope diffraction through the SWS output (Beintema 1999). The telescope PSF model includes the primary mirror, the secondary mirror and its support structure with the central obscuration disk being determined by the outer edge of the secondary baffle. This PSF is convolved first with the SWS entrance slit, and then

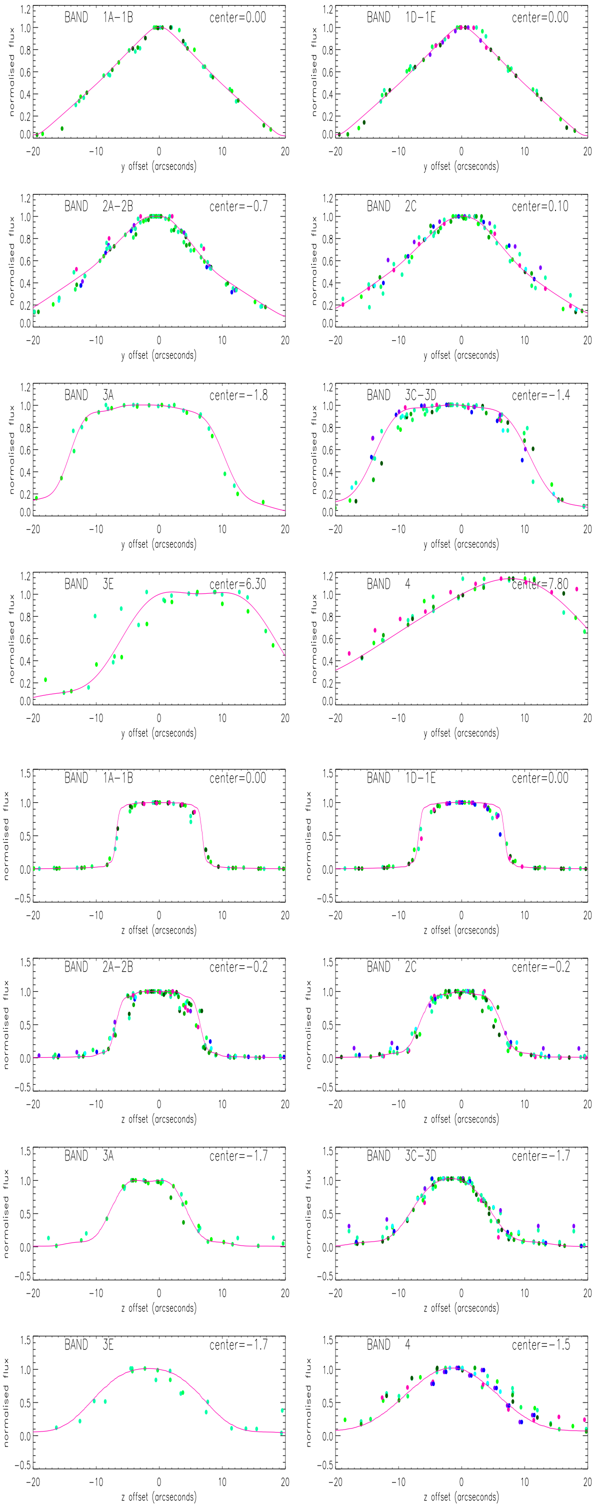

Figure 2. SWS Beam profile model (continuous line), compared with the beam profile calibration data (dots), along the cross-dispersion direction Y (four upper panels) and dispersion direction Z (four lower panels.

with the detector response profile, empirically determined from calibration observations. Its shape has been found to be triangular in the cross-dispersion direction, fact attributed to imaging defects inside the SWS. The beam profile model also takes into account the internal detector misalignments determined from the beam profile calibration observations. Model and beam profile data agree reasonably well. For completeness in these proceedings, cross-section cuts of the profiles are shown in Figure 2. The SWS beam profiles are normalised to unity at the position at which the point source flux has been calibrated, therefore the conversion factors from point to extended source flux are directly obtained by integrating the profiles, according to Equation 1. These are listed in Table 5. The SWS beam profiles are planned for inclusion in OLP9.5 and OSIA 2.0 as standalone calibration files.

Table 5. SWS Flux conversion factors for extended sources

AOT Band	Wavelength (μm)	Jy to MJy sr^{-1}
1A	2.48	139
1B	2.87	134
1D	3.08	132
1E	3.8	132
2A	4.7	115
2B	5.9	118
2C	7.7	117
2C´	11	114
3A	14	107
3C	17	105
3D	20	97
3E	28.5	65
4	30.9	45
4´	40	42

ACKNOWLEDGMENTS

This paper is based on the results discussed within the ISO Beam Profile and Pointing Calibration Working Group, chaired by the author, to which the main contributors are D. Beintema, R. Laureijs, C. Lloyd, R. Lorente, K. Okumura, A. Pollock and B. Schulz.

REFERENCES

Beintema, D. A., 1999, In SWS Interactive Analysis.
Gry, C., et al., 2000, The LWS Handbook.
Laureijs, R., 1999, ISO PHT Explanatory Library.
Laureijs, R., et al., 2000, The PHT Handbook.
Lloyd, C., 2000, These proceedings.
Müller, Th., 2000, These proceedings.
Okumura, K., 2000, These proceedings.
Salama, A., 1998, ISO SWS Explanatory Library.
Siebenmorgen, R., et al., 2000, The CAM Handbook.